Clinical and Genetic Spectrum of Children with Primary Ciliary Dyskinesia in China

Zhuoyao Guo, MD[1,†], Weicheng Chen, MD, PhD[2,†], Libo Wang, MD[1], and Liling Qian, MD, PhD[1]

Objective To report detailed knowledge about the clinical manifestations, ciliary phenotypes, genetic spectrum as well as phenotype/genotype correlation in primary ciliary dyskinesia (PCD) in Chinese children.

Study design We recruited 50 Chinese children with PCD. Extensive clinical assessments, nasal nitric oxide, high-speed video analysis, transmission electron microscopy, and genetic testing were performed to characterize the phenotypes and genotypes of these patients.

Results Common clinical features included chronic wet cough (85.4%), laterality defects (70.0%), and neonatal respiratory distress (55.8%). A high prevalence of congenital abnormalities (30.2%, 13/43), observed in patients who underwent comprehensive examination for comorbidities, included thoracic deformity (11.6%, 5/43), congenital heart disease (9.3%, 4/43), and sensorineural deafness (2.3%, 1/43). For 24 children age >6 years, the mean predicted values of forced expiratory volume in 1 second were 87.2%. Bronchiectasis evident on high-resolution computed tomography was reported in 38.1% of patients (16/42). Biallelic mutations (81 total; 57 novel) were identified in 13 genes: *DNAAF3, DNAAF1, DNAH5, DNAH11, CCDC39, CCDC40, CCDC114, CCDC103*, *HYDIN, CCNO*, *DNAI1, OFD1*, and *SPAG1*. Overall, ciliary ultrastructural and beat pattern correlated well with the genotype. However, variable phenotypes were also observed in *CCDC39* and *DNAH5* mutant cilia.

Conclusions This large PCD cohort in China broadens the clinical, ciliary phenotypes, and genetic characteristics of children with PCD. Our findings are roughly consistent with previous studies besides some peculiarities such as high prevalence of associated abnormalities. *(J Pediatr 2020;225:157-65)*.

Primary ciliary dyskinesia (PCD, Online Mendelian Inheritance in Man: 244400) is an orphan, autosomal-recessive or X-linked disease characterized by abnormal motile ciliary function.[1] As a consequence, PCD often presents a variety of clinical manifestations, such as upper and lower airway infection, laterality defects, and infertility.[2] The estimated prevalence of PCD is 1:10 000 to 1:40 000 in live-born children.[3]

Currently, there is no single "gold standard" diagnostic test. The European Respiratory Society recommended that diagnosis requires access to a diversity of technically demanding methods, including nasal nitric oxide (nNO), high-speed video analysis (HSVA), transmission electron microscopy (TEM), and genetic testing.[4] It has been reported that inner dynein arms (IDA) defects, combined with microtubular disarrangement (MTD), many of which are associated with biallelic mutations in *CCDC39* and *CCDC40*, have worse pulmonary function,[5] whereas mutations in *RSPH1* are usually associated with higher nNO and milder clinical disease.[6] As an easy, inexpensive, and expeditious diagnostic tool for establishing PCD diagnosis, HSVA is proposed as the first-line test and increasingly applied.[4] However, the relationships between clinical manifestations, ciliary ultrastructural defect, genotype, and ciliary beat pattern have not been well established.

Because of the lack of awareness of PCD and the diagnostic methods, the disease is underdiagnosed in China. Currently, limited data are available on the comprehensive description of characteristics or genotypic spectrum in Chinese children. Until now, only 19 Chinese cases (including adult patients) have been reported, in which pathogenic variants were identified.[7-15] In our center, a multidisciplinary team of clinical and laboratory staff determines whether patients have PCD, using clinical history, nNO, HSVA, TEM, and genetic analysis. In the present study, we systematically evaluated the clinical symptoms, ciliary phenotype, and genetic spectrum, as well as the diagnostic characteristics of Chinese children with PCD, who were followed up

CA	Central apparatus	HTX	Heterotaxy
cDNA	Complementary DNA	IDA	Inner dynein arms
FEV_1	Forced expiratory volume in the first second	MTD	Microtubular disarrangement
		nNO	Nasal nitric oxide
FVC	Forced vital capacity	ODA	Outer dynein arms
HGMD	Human Gene Mutation Database	PCD	Primary ciliary dyskinesia
HRCT	High-resolution computed tomography	SIT	Situs inversus totalis
		SS	Situs solitus
HSVA	High-speed video analysis	TEM	Transmission electron microscopy

From the [1]Respirology Department, Children's Hospital of Fudan University, Shanghai, P.R. China; and [2]Cardiothoracic Surgery Department, Children's Hospital of Fudan University, Shanghai, China

†Contributed equally.

Supported by Shanghai Science and Technology Commission's Scientific and Technological Innovation Action Plan (No. 16411950700), and the National Natural Science Foundation of China (No.81671502). The authors declare no conflicts of interest.

https://doi.org/10.1016/j.jpeds.2020.05.052

at our center. At the same time, the associations between ciliary beat patterns, ultrastructural defects, and genotypes were also comprehensively determined.

Methods

Patients with symptoms suggestive of PCD, with at least 2 out of 4 key clinical features (laterality defects, unexplained neonatal respiratory distress, year-round daily cough, or nasal congestion) or siblings of confirmed patients were prospectively screened between January 1, 2016 and January 1, 2019 at the Children's Hospital of Fudan University. These patients underwent a standardized diagnostic protocol, including HSVA, TEM, nNO, and genetic testing. The diagnosis of PCD was made according to the European Respiratory Society guidelines.[4] Confirmed PCD diagnosis required a hallmark ultrastructural defect (ie, dynein arm [DA] defect, outer dynein arms [ODA] defect, IDA defect with MTD, and/or nonambiguous biallelic mutations in PCD-causing genes). Demographic information, laboratory results including sputum culture, computed tomography, echocardiography, abdominal ultrasound, and pulmonary function test were obtained when enrolled.

Measurement of nNO

nNO testing was performed using an EcoMedics CLD88 chemiluminescence NO analyser (Duernten, Switzerland); the measurement of nNO in cooperative children was performed by breath hold maneuver as described previously.[16] For children uncooperative (usually less than 5 years old), nasal sampling was performed for 60 seconds during tidal breathing.[17] Results were reported in nL/min with the following equation: nNO (nL/min) = NO (ppb) × sampling rate (mL/min).

Transmission Electron Microscopy Examination

Samples of nasal mucosa were fixed in 2.5% glutaraldehyde, and ciliary ultrastructural analysis was carried out by TEM (JEM-1400; Jeol, Tokyo, Japan). TEM was performed as previously described.[11] Briefly, the nasal mucosa was fixed with glutaraldehyde (2.5% w/v) in 0.1 M sodium cacodylate buffer. Following fixation in osmium tetroxide (1% w/v), samples were dehydrated through graded ethanol series and embedded in epoxy resin. Sections were cut at 50-70 nm thickness and stained with 2% methanolic uranyl acetate and Reynold's lead citrate for analysis.

High-Speed Video Microscopy Analysis

Nasal tissue was suspended in L-15 medium (Invitrogen, Carlsbad, California). Cilia beat frequency and pattern were recorded at 200 frames/seconds at room temperature (25°C) by a Leica inverted microscope (Leica DMI3000B, Solms, Germany) as described.[11] HSVA was carried out directly after brushing. The digital recordings were evaluated in a blinded fashion by 2 investigators. To evaluate the abnormalities in ciliary motion, we examined the ciliary beat pattern by using slow motion playback of the video sequence to generate tracings of the ciliary beat; at least 10 edges were analyzed per subject. The ciliary beat pattern was described as follows: normal, immotile, minimal residual movements stiff, restricted, and circular. Repeated nasal brushing was conducted for ciliary ultrastructure and function analysis, when initial results were insufficient or inconclusive.

Whole Exome Sequencing and Sanger Sequencing Validation

Genomic DNA was isolated from the peripheral blood of the probands and available family members, using the QIAamp DNA Blood Mini kit (Qiagen, Hilden, Germany). Whole exome sequencing was performed to search for potential genetic defects at the molecular genetic diagnosis center of Fudan University as previously described.[18] Briefly, whole exomes were captured using an Agilent SureSelect Human All ExonV5 Kit (Agilent, Santa Clara, California) and sequenced on an Illumina HiSeq 2000 platform. The sequencing reads were aligned to the human reference genome (UCSC hg19) with Burrows-Wheelchair Aligner v 0.7.9a. After quality control, variants were annotated by Variant Effect Predictor (http://asia.ensembl.org/index.html) and ANNOVAR (http://www.openbioinformatics.org/annovar) and compared computationally with the list of reported pathogenic variations from the Human Gene Mutation Database (HGMD, professional version). For variations that are not reported pathogenic in the HGMD, our own databases and the Exome Aggregation Consortium, 1000 Genome Project, Genome Aggregation Database, and Single Nucleotide Polymorphism Database were used to filtering out common variants (minor allele frequency >1%). Intronic variants, synonymous variants were also discarded. The protein functional consequence of variants were assessed with SIFT, Provean, PolyPhen2, and MutationTaster.[11] We evaluated the pathogenicity of the candidate variants based on the American College of Medical Genetics and Genomics guideline.[19] Sanger sequencing was further performed to validate the candidate variants, and segregation analyses were performed in family members.

Complementary DNA Analysis

To determine the effect of the noncanonical splice variant on transcripts, reverse transcription-polymerase chain reaction was employed, using RNA from nasal epithelial cells. Total RNA from nasal cell suspensions was isolated using RNeasy Mini Kit (Qiagen, Germany). Conversion of RNA to complementary DNA (cDNA) was performed with the first-strand cDNA synthesis kit (Takara, Dalian, China), according to manufacturer's instructions. cDNA was amplified by polymerase chain reaction with specific primers, and the product was subjected to 2% agarose gel electrophoresis and sequence analyses. The primers used in polymerase chain reaction reactions are listed in **Table I** (available at www.jpeds.com).

Statistical Analyses

Statistical analysis was performed using Microsoft Excel (Microsoft, Redmond, Washington) and SPSS v 22 (IBM

Corporation, Armonk, New York). The differences between rates were tested by χ^2 or Fisher exact tests. Group comparisons were performed using the Student *t* testing. Statistical tests were 2-sided and statistical significance was accepted at $P < .05$

Ethical Considerations

The study protocol was approved by the Ethics Committees of Children's Hospital of Fudan University.

Results

A total of 72 children, suspected of PCD, were invited to participate, and of these, 18 children no longer fulfilled inclusion criteria, and 4 were "inconclusive" after assessments by a state-of-the-art battery of diagnostic tests. Finally, 50 patients with PCD from 47 families were confirmed with a positive diagnosis of PCD and enrolled (**Figure 1**; available at www.jpeds.com). The frequency of clinical characterizations is summarized in **Table II**. Among them, 27 (54.0%) were male, and consanguineous marriage was found for 2 patients. The mean age at enrollment was 8.9 years (range 0.3-18.0); mean age at diagnosis was 8.1 years (range 0-18.0); 15 (30.0%) patients had situs solitus (SS), 32 (64.0%) had situs inversus totalis (SIT), and 3 (6.0%) had heterotaxy (HTX). Nasosinusitis was detected in 100.0% of patients who underwent sinus computed tomography (CT) (42/42). Other common clinical features include chronic otitis media (96.8%, 30/31), chronic wet cough (85.4%, 41/48), and laterality defects (70.0%, 35/50). Twenty-four children (55.8%) had a specific history of an unexpected neonatal respiratory syndrome.

Respiratory cultures were obtained from 32 of these patients. The samples were expectorated sputum in 72% and pharyngeal swabs in 28%. The median number of bacterial culture for each patient was 4 (range 1-13). The most common bacterial isolates were *Haemophilus influenza* (18.8%, 6/32), *Pseudomonas aeruginosa* (12.5%, 4/32), and *Moraxella catarrhalis* (9.4%, 3/32); *Staphylococcus aureus* (6.3%, 2/32), *Acinetobacter baumannii* (3.1%, 1/32), and *Legionella pneumophila* (3.1%, 1/32) were relatively less common.

Twenty-four children, older than 6 years, underwent pulmonary function test at diagnosis. Reductions of forced expiratory volume in the first second (FEV_1) (mean ± SD: 87.2 ± 9.8% predicted) and forced vital capacity (FVC) (83.2% ± 17.3% predicted) were observed in these children, and forced expiratory flow at 25% and 75% of the pulmonary volume ($FEF_{25\%–75\%}$) was also significantly affected (49.1% ± 20.4% predicted).

High-resolution computed tomography (HRCT) was available in 42 patients (images are available on request), which revealed bronchiectasis in 38.1% of the children, and 7 (16.7%) had no apparent change in HRCT imaging. The mean age (years ± SD) for those with bronchiectasis was significantly greater than for those without (13.6 ± 5.6 vs 5.8 ± 5.7, $P < .05$). The median number of lobes involved was 2.4, and the right middle lobe or left middle lobe was the most common lobe to manifest bronchiectasis (data not shown). Diffuse nodules were frequently observed (52.4%, 22/42).

A high prevalence of congenital abnormalities (30.2%, 13/43) in PCD was observed in patients who underwent comprehensive examination for comorbidities. A considerable proportion of cases with PCD had thoracic deformity (11.6%, 5/43) and congenital heart disease (9.3%, 4/43). There were also many other conditions identified in these children with PCD, including scoliosis, anosmia, congenital deafness, dwarfism, and antineutrophil cytoplasmic

Table II. Clinical and demographic data from patients with PCD

Parameters	All	SIT/HTX (70.0%, 35/50)	SS (30.0%, 15/50)	*P* value
Male sex*, %	54.0 (27/50)	51.4 (18/35)	60.0 (9/15)	.76
Age, y	8.9	9.5	7.5	.30
NRDS*, %	55.8 (24/43)	53.6 (15/28)	60.0 (9/15)	.69
Chronic wet cough*, %	85.4 (41/48)	90.9 (31/33)	73.3 (11/15)	.18
Nasosinusitis*, %	100 (42/42)	100 (30/30)	100 (12/12)	/
Chronic otitis media*, %	96.8 (30/31)	95.5 (21/22)	100 (9/9)	1.00
Hearing loss*, %	66.7 (22/33)	59.0 (13/22)	81.8 (9/11)	.26
FEV_1,% pred	87.2	86.9	87.7	.95
Bronchiectasis*, %	38.1 (16/42)	46.4 (13/28)	21.4 (3/14)	.18
Ciliary defect type*, %	ODA/IDA; ODA; MTD/IDA/CA; CA; Normal;	ODA/IDA; ODA; MTD/IDA/CA; Normal;	ODA/IDA; ODA; MTD/IDA/CA; CA; Normal;	
Gene	*DNAH5;DNAHI1; CCDC40;CCDC39; CCNO;CCDC114; CCDC103;DNAAF3; SPAG1;OFD1;DNAI1; DNAAF1;HYDIN*	*DNAH5;DNAHI1; CCDC40;CCDC39; CCDC103;DNAI1; SPAG1;OFD1; DNAAF3; DNAAF1;*	*DNAH5;DNAHI1; CCDC40; CCDC39;CCNO;CCDC114; HYDIN;*	

NRDS, neonatal respiratory distress.
Group comparisons were performed using the χ^2 test or Fisher exact tests.
*Numerator/denominator, positive cases/total number of patients who underwent corresponding inspection.

autoantibody-associated vasculitis. Detailed demographic and clinic manifestations are shown in **Table III** (available at www.jpeds.com).

Measurement of nNO

The nNO value in 29 cooperative children ranged from 5.6 to 113.2 nL/minute, with a median of 13.9 nL/minute. Although the nNO value in 10 uncooperative children ranged from 1.4 to 37.8 nL/minute, with a median of 10.5 nL/minute. Of the 39 patients tested, 38 (97.4%) were far below the recommended diagnostic cut-off (77.0 nL/minute for oral exhalation against resistance, 47.4 nL/minute for tidal breathing[20]) (**Table IV**).

Ciliary Structural and Functional Analysis

Out of 46 individuals, 33 (71.7%) had definitely abnormal ciliary ultrastructure, including ODA defects (23.9%, 11/46) (**Figure 2**, A; available at www.jpeds.com), combined ODA and IDA defects (21.7%, 10/46) (**Figure 2**, B; available at www.jpeds.com), DA defects combined with microtubular disarrangement (19.6%, 9/46) (**Figure 2**, C; available at www.jpeds.com), and central apparatus (CA) defects (2/46, 4.3%) (**Figure 2**, D; available at www.jpeds.com). High-speed video microscopy revealed that among the 44 individuals, 42 (95.5%) had abnormal ciliary beat pattern, including virtually immotile (56.8%, 25/44) (**Video 1**; available at www.jpeds.com), stiff (18.2%, 8/44)

Table IV. Detailed ultrastructural defects and genetic spectrum in subgroups with different CBP

Cases	nNO(nL/min)	TEM	CBP	CBF(Hz)	Gene
P09	10.3	ODA/IDA	Immotile	0	*DNAH5*
P12	12.2	ODA	Immotile	0	*DNAH5*
P21	5.6	ODA	Immotile	0	*DNAH5*
P31	12.3	Inconclusive	Immotile	0	*DNAH5*
P40	13.5	ODA	Immotile	0	*DNAH5*
P42	14.7	ODA	Immotile	0	*DNAH5*
P05	10.4	Inconclusive	Minimal residual movements	0	*DNAH5*
P11	9.1	ODA/IDA	Minimal residual movements	0	*DNAH5*
P14	6.6	ODA	Minimal residual movements	0	*DNAH5*
P49	13.2	Inconclusive	Minimal residual movements	0	*DNAH5*
P24	29.5	NA	Restricted	5.1	*DNAH5*
P35	NA	ODA	NA	NA	*DNAH5*
P36	NA	ODA	NA	NA	*DNAH5*
P25	10.5	Normal	Nearly normal	9.09	*DNAH11*
P32	5.1	Inconclusive	Nearly normal	8.42	*DNAH11*
P17	8.5	Normal	Restricted	11.11	*DNAH11*
P23	7.8	NA	Restricted	10.2	*DNAH11*
P30	NA	Normal	Restricted	10.3	*DNAH11*
P44	37.8	Normal	Restricted	7.8	*DNAH11*
P45	113.2	Normal	Restricted	6.9	*DNAH11*
P28	NA	NA	Restricted	9.97	*DNAH11*
P04	16.7	MTD/IDA/CA	Stiff	NA	*CCDC39*
P33	15.1	MTD/IDA/CA	Stiff	NA	*CCDC39*
P13	12.6	MTD/IDA/CA	Immotile	0	*CCDC39*
P29	NA	Inconclusive	NA	NA	*CCDC39*
P02	21.0	MTD/IDA/CA	Stiff	NA	*CCDC40*
P18	8.7	MTD/IDA/CA	Stiff	11.76	*CCDC40*
P22	7.8	MTD/IDA/CA	Stiff	9.02	*CCDC40*
P26	18.2	NA	Stiff	NA	*CCDC40*
P34	33.2	MTD/IDA/CA	Stiff	4.46	*CCDC40*
P46	9.6	MTD/IDA/CA	Minimal residual movements	0	*CCDC40*
P01	NA	ODA/IDA	Immotile	0	*DNAAF3*
P03	16.3	Inconclusive	Immotile	0	*DNAAF3*
P06	11.7	ODA/IDA	Immotile	0	*DNAAF3*
P16	1.4	ODA/IDA	Immotile	0	*DNAAF3*
P43	3.4	ODA/IDA	Immotile	0	*DNAAF3*
P38	NA	Normal/CA	Circular	NA	*HYDIN*
P39	NA	Normal/CA	Circular	NA	*HYDIN*
P08	9.5	ODA	Immotile	0	*CCDC103*
P07	12.1	Inconclusive	Minimal residual movements	2.1	*CCDC114*
P41	15.1	No cilia	NA	NA	*CCNO*
P50	NA	ODA/IDA	NA	NA	*SPAG1*
P47	14.0	Inconclusive	Immotile	0	*DNAAF1*
P37	6.8	ODA	Minimal residual movements	0	*DNAI1*
P48	6.2	MTD/DA	Stiff	5.5	*OFD1*
P10	18.3	ODA	Immotile	0	WES(−)
P15	18.1	ODA/IDA	Minimal residual movements	0	WES(−)
P20	NA	ODA/IDA	Minimal residual movements	0	WES(−)
P19	10.7	ODA/IDA	Immotile	0	NA
P27	NA	ODA	NA	NA	NA

WES, whole exome sequencing.

(**Video 2**; available at www.jpeds.com), restricted (15.9%, 7/43) (**Video 3**; available at www.jpeds.com), and circular (4.5%, 2/44) (**Video 4**; available at www.jpeds.com). Ciliary beat frequency was available in 38 children with PCD. Frequencies ranged from 0.0 to 11.76 Hz with a median frequency of 2.89 Hz; 8 patients had ciliary beat frequencies within the normal range of 8.42-11.76 Hz (mean 9.98 Hz); 5 individuals had obviously reduced beat frequency 2.46-7.80 Hz (mean 5.95 Hz), whereas cilia in the other 25 children were nearly or completely immotile. The summary of diagnostic accuracy of nasal nitric oxide, transmission electron microscopy and high-speed video analysis in children with PCD are shown in **Table V** (available at www.jpeds.com).

Genetic Characteristics and cDNA Analysis

Collectively, 81 biallelic mutations spanning 13 genes were identified from 48 subjects with PCD of 46 families. Among the 81 variants, 29 were missense variants, 24 were frameshift, 18 were nonsense variants, and 10 were splicing variants; 57 of 81 variants (70.4%) were novel; 5 subjects exhibited homozygous mutations and 40 exhibited compound heterozygous mutations (**Table VI**). Interestingly, in P33, we identified a noncanonical splice variant c.931-8T>C in trans with a frameshift variant c.2447_2448delCA, p.T816Kfs*3 in *CCDC39*. c.931-8T>C was not predicted to have a splicing effect but was demonstrated to induce an aberrant splicing at messenger RNA level (**Figure 3**; available at www.jpeds.com) by sequencing of messenger RNA from the patient's nasal epithelial cells.

The Correlation between Clinical Characteristics, Ciliary Phenotypes, and Genetic Spectrum

The clinical and genetic pictures of patients with PCD caused by different ciliary beat pattern are shown (**Table VII**). Generally speaking, ciliary ultrastructural defects and ciliary beat pattern correlated well with genotypes. It is worth noting that the different ciliary beat patterns were identified within 1 gene (**Table IV**). Prevalence of clinical manifestations did not differ for SIT/HTX group vs the SS groups. Our data did not show any significant difference in the distribution of ciliary phenotypes and genetic spectrum between the SIT/HTX and the SS groups (**Table II**).

Discussion

In the present study, we analyzed a large cohort of children with PCD in China. We robustly and comprehensively examined multiple aspects of PCD characteristics, including clinical manifestations, ciliary phenotype, as well as genetic characterization in these subjects, and gained initial insights into the features of PCD in China.

As expected, the clinical manifestations of patients with PCD in China is similar to that previously described, with high prevalence of nasosinusitis, otitis media, chronic wet cough, and RDS. In the present study, laterality defect was reported in 70.0% of subjects, which is significantly higher than the proportion reported in Europe and America.[21,22] The roster of pathogens, isolated from our patients, was similar to that from previous studies,[23,24] and included *Haemophilus influenza*, *Pseudomonas aeruginosa*, *Moraxella catarrhalis*, and *Staphylococcus aureus*. It is worth mentioning that compared with the high prevalence of *Haemophilus influenza* (22%-80%), and *Pseudomonas aeruginosa* (15%-47%), reported previously,[25-28] the incidence is markedly lower in our patients.

A few studies have assessed the onset and progression of lung disease in early childhood PCD; Brown et al, for instance, reported that bronchiectasis could in fact occur in infants.[29] In the present study, HRCT was performed in 11 children <4 years of age and revealed that 53.1% had normal lung structure, while patchy exudation and lobar atelectasis instead of bronchiectasis were identified in the rest. In our study, the percentage of bronchiectasis rose with increasing age. Overall, our results revealed that the lung damage of patients with PCD increased with age, which highlights the importance of early diagnosis and aggressive early management.

A previous cross-sectional study in 158 children with PCD showed that mean FEV_1 was 82.5%, predicted at mean age 8.7 years.[26] In another multicenter study of 137 children (7.8 ± 4.6 years old) with PCD, percent predicted FEV_1 was 82.7%, and declined significantly over time (mean −0.57 percent predicted per year).[27] In general, there was a significant relationship between age and lung disease progression.[27,30] Compared with Caucasian pediatric cohorts, the lung function of our patients is significant higher, as the mean FEV_1 is 87.2% predicted at an older age of 11 years.

Recently, strong correlations between genotype-phenotype relationships have been identified in PCD[5,6,27]; specifically, patients who had biallelic mutations in *CCDC39* or *CCDC40* had worse lung disease and presented with it earlier. In our study, a considerable proportion of patients carried mutations in *CCDC39/CCDC40* (20.8%, 10/48). Among them, 3 patients (P2, P18 and P33) presented with mild lung disease by both functional and structural assessment (spirometry and CT scans). Intriguingly, P18, the younger sister of P2, had near normal lung function and structure at age 7 years. These findings highlight the significant heterogeneity of pulmonary involvement, which challenges the recognition of PCD. *OFD1* has long been recognized as the gene implicated in the primary ciliopathies, which are characterized with neurologic findings, dysmorphic features, and skeletal symptoms (digital, facial, or dental). Variants affecting the C-terminal part of *OFD1* (exons 16-22) were found to be associated with X-linked PCD without co-morbidities,[31] which is exactly the case for P48 (exons 21) in our study. Further study is needed to better elucidate the heterogeneous phenotype.

Cilia motility not only plays a key role in mucociliary transport but may be responsible for creating a leftward flow pattern at the embryonic node, which is key to a properly arranged, asymmetric cardiovascular system. Thus, there

Table VI. Details of mutations identified in Chinese children with PCD

Patients	Gene	cDNA position	Zygosity	Type of variants	Effect on protein	Ref(PMID)/HGMD/ClinVar
P1	*DNAAF3*	NM_001256714.1:c.388_432 + 60del	Comp.	Splice-site	/	31186518
		NM_001256714.1: c.811_815dupGACGC	Het	Frameshift	p.A273Tfs*13	31186518
P2	*CCDC40*	NM_001243342: c.3224T>C	Comp.	Missense	p.L1075P	/
		NM_001243342: c.901C>T	Het	Nonsense	p.R301*	/
P3	*DNAAF3*	NM_001256714.1: c.442delC	Comp.	Frameshift	p.L148Wfs*13	31186518
		NM_001256714.1: c.1465C>T	Het	Nonsense	p.Q489*	31186518
P4	*CCDC39*	NM_181426:c. 1819A>T	Comp.	Nonsense	p.K607*	/
		NM_181426:c.2447_2448delCA	Het	Frameshift	p. T816Kfs*3	/
P5	*DNAH5*	NM_001369:c.278-1_295delinsACAACAACAA	Comp.	Splice-site	/	/
		NM_001369: c.6304C>T	Het	Missense	p.R2102C	Pathogenic
P6	*DNAAF3*	NM_001256714.1:c.679delC	Hom	Frameshift	p.L227Sfs*28	31186518
P7	*CCDC114*	NM_144577:c.705_706 insGCAG	Comp.	Frameshift	p.P236Afs*11	/
		NM_144577:c.-41-2A>C	Het	Splice-site	/	/
P8	*CCDC103*	NM_001258395:c.170_175delAGCCACinsGG	Hom	Frameshift	/	/
P9	*DNAH5*	NM_001369:c.7579_7590del	Comp.	Frameshift	p.2527_2530del	/
		NM_001369:c.5146C>T	Het	Missense	p.R1716W	19357118
P10	WES (–)	/	/	/	/	/
P11	*DNAH5*	NM_001369:c.6647delA	Comp.	Frameshift	p.K2216Rfs*20	/
		NM_001369: c.7523T>C	Het	Missense	p.L2508P	
P12	*DNAH5*	NM_001369: c.6139C>T	Comp.	Nonsense	p.Gln2047*	/
		NM_001369: c.1852C>T	Het	Nonsense	p.Arg618*	29363216
P13	*CCDC39*	NM_181426:c.526_527delCT	Hom	Frameshift	p.L176Afs*10	23255504
P14	*DNAH5*	NM_001369: c.7469G>A	Comp.	Nonsense	p.W2490*	/
		NM_001369: c.9235C>T	Het	Nonsense	p.R3079*	/
P15	WES (–)	/	/	/	/	/
P16	*DNAAF3*	NM_001256714.1: c.200C>A	Comp.	Missense	p.S67Y	31186518
		NM_001256714.1: c.811_815dupGACGC	Het	Frameshift	p.A273Tfs*13	31186518
P17	*DNAH11*	NM_001277115:c.7292G>T	Comp.	Missense	p.S2431I	/
		NM_001277115:c.7364A>C	Het	Missense	p.D2455A	/
		NM_001277115:c.9017C>T	/	Missense	p.T3006M	/
		NM_001277115:c.13373C>T	/	Missense	p.P4458L	22184204; 29997923
P18	*CCDC40*	NM_001243342: c.3224T>C	Comp.	Missense	p.L075P	/
		NM_001243342: c.901 C>T	Het	Nonsense	p.R301*	/
P19	/	/	/	/	/	/
P20	WES (–)	/	/	/	/	/
P21	*DNAH5*	NM_001369: c.4193A>G	Hom	Missense	p.Q1398R	/
P22	*CCDC40*	NM_001243342: c.1159+1G>T	Comp.	Splice-site	/	/
		NM_001243342: c.50C>G	Het	Missense	p.S17W	/
P23	*DNAH11*	NM_001277115:c.9539T>A	Comp.	Nonsense	p.L3180*	/
		NM_001277115:c.9706C>T	Het	Nonsense	p.R3236*	Pathogenic
P24	*DNAH5*	NM_001369: c.13126-2A>G	Comp.	Splice-site	/	/
		NM_001369: c.7789A>G	Het	Missense	p.T2597A	/
P25	*DNAH11*	NM_001277115:c.3020T>G	Comp.	Nonsense	p.L1007 *	/
		NM_001277115:c.3470T>G	Het	Missense	p.L1157R	/
P26	*CCDC40*	NM_001243342: c.1345C>T	Comp.	Nonsense	p.R449*	21131974; 25525159
		NM_001243342: c.2446delG	Het	Frameshift	p.E816Kfs*18	/
P27	/	/	/	/	/	/
P28	*DNAH11*	NM_001277115:c.2485C>T	Comp.	Missense	p.R829C	/
		NM_001277115:c.5608C>T	Het	Missense	p.P1870S	/
P29	*CCDC39*	NM_181426:c.732_733del	Hom	Frameshift	p.A245Ffs*18	/
P30	*DNAH11*	NM_001277115:c.7292G>T	Comp.	Missense	p.S2431I	/
		NM_001277115:c.7364A>C	Het	Missense	p.D2455A	/
		NM_001277115:c.9017C>T	/	Missense	p.T3006M	/
		NM_001277115:c.13373C>T	/	Missense	p.P4458L	22184204; 29997923
P31	*DNAH5*	NM_001369: c.5563dupA	Comp.	Frameshift	p.I1855Nfs*6	11788826; 26228299
		NM_001369: c.13724-1G>C	Het	Splice-site	/	/
P32	*DNAH11*	NM_001277115: c.4457T>A	Comp.	Missense	p.L1486Q	/
		NM_001277115:c.10006G>T	Het	Missense	p.A3336S	/
P33	*CCDC39*	NM_181426:c.2447_2448del	Comp.	Frameshift	p.T816Kfs*3	/
		NM_181426:c.931-8T>C	Het	Splice-site	/	/
P34	*CCDC39*	NM_181426:c.2670-1G>A	Comp.	Splice-site	/	/
		NM_181426:c.2542G>T	Het	Nonsense	p.E848*	/
P35	*DNAH5*	NM_001369: c.9897+1G>A	Comp.	Splice-site	/	/
		NM_001369: c.8265C>G	Het	Missense	p.F2755L	/
P36	*DNAH5*	NM_001369: c.8030G>A	Comp.	Missense	p.R2677Q	24150548
		NM_001369: c.5150T>A	Het	Missense	p.F1717Y	/
P37	*DNAI1*	NM_001281428:c. 180 G>A	Comp.	Missense	c.G180A	/
		NM_001281428:c.1403_1404delTG	Het	Frameshift	p. L468Rfs*14	/
P38	*HYDIN*	NM_001270974:c.7158+1G>A	Comp.	Splice-site	/	/
		NM_001270974:c.211C>T	Het	Nonsense	p.R71*	/

(*continued*)

Table VI. Continued

Patients	Gene	cDNA position	Zygosity	Type of variants	Effect on protein	Ref(PMID)/HGMD/ClinVar
P39	*HYDIN*	NM_001270974:c.7158+1G>A	Comp.	Splice-site	/	/
		NM_001270974:c.211C>T	Het	Nonsense	p.R71*	/
P40	*DNAH5*	NM_001369: c. 8498 G>A	Comp.	Missense	p.R2833H	23891469; 27637300
		NM_001369: c.1616_1617delAG	Het	Frameshift	p.E539Vfs*6	/
P41	*CCNO*	NM_021147:c.615delC	/	Frameshift	p.C205Wfs*64	/
		NM_021147:c.253_262dupGGCCCGGCCC	/	Frameshift	p. Q88Rfs*51	/
P42	*DNAH5*	NM_001369: c.5563dupA	Comp.	Frameshift	p.I1855Nfs*6	11788826
		NM_001369: c.4147_4148delAinsTCC	Het	Frameshift	p.I1383Sfs*22	/
P43	*DNAAF3*	NM_001256714.1:c.1030 G> T	Comp.	Missense	p.D344Y	/
		NM_001256714.1:c.557 G >A	Het	Missense	p.G186E	/
P44	*DNAH11*	NM_001277115:c. 2406 G>A	Comp.	Nonsense	p.W802*	31040315
		NM_001277115:c.846 G>C	Het	Missense	p.M282I	31040315
P45	*DNAH11*	NM_001277115:c.3470 T>G	Comp.	Missense	p.L1157R	28492532
		NM_001277115:c.6727 C>G	Het	Missense	p.R2243G	28492532
P46	*CCDC39*	NM_181426:c.1819 A> T	/	Nonsense	p.K607*	/
		NM_181426:c.286C>T	/	Nonsense	p.R96*	Pathogenic
P47	*DNAAF1*	NM_178452:c.376delG	Comp.	Frameshift	p.E126Kfs*35	/
		NM_178452:c.1801_1804del	Het	Frameshift	p.D601Lfs*45	/
P48	*OFD1*	NM_003611:c.2852delC	Hem	Frameshift	p.S951Lfs*8	/
P49	*DNAH5*	NM_001369:c. 9502 C>T	Comp.	Nonsense	p.R3168*	Pathogenic
		NM_001369:c. 7912 A> T	Het	Nonsense	p.K2638*	/
P50	*SPAG1*	NM_172218: c.1649_1650insA	Comp.	Frameshift	p. D551Rfs*9	/
		NM_172218:c.691delT	Het	Frameshift	p. Y231Ifs*12	/

Comp., compound; *Het*, heterozygous; *PMID*, PubMed Unique Identifier.

is a considerable proportion of patients with PCD (3.6% −17.1%) also with CHD.[21,22,32,33] Consistent with the literature, 8% of the children with PCD were diagnosed with CHD in our study. Apart from CHD, certain extracardiac anomalies have been observed in our study. These comorbidities, such as anosmia, sensorineural deafness, and skeletal dysplasia were also reported in some case reports. A high (9%) prevalence of pectus excavatum was also identified by Kennedy et al.[34] Intriguingly, these phenotypes are common in primary ciliopathies. By whole exome sequencing, we did not found any other potential genes that might explain these comorbidities. Thus, it remains uncertain whether these are coincidental findings or innate aspects of both PCD and primary ciliopathies. Further research is needed to identify the connection and elucidate the underlying molecular mechanisms of phenotypic overlap. Overall, however, little focus has been devoted to the associated abnormalities in PCD comprehensively.[21] Nonrespiratory conditions may complicate PCD care, contribute to the progression of the disease, and alter the response to treatment. Given the high prevalence of associated abnormalities identified in this study, we recommend that all patients diagnosed with PCD have a comprehensive valuation for extrapulmonary findings.

Our study has identified correlations among ciliary ultrastructural defects, genotypes and ciliary beat pattern, as follows: (1) Immotile cilia usually showed ODA absence or ODA/IDA absence. Genes encoding proteins of the ODAs, ODA docking

Table VII. Clinical data, ciliary ultrastructural defects, and genetic characteristics of PCD according to CBP

Parameters	All	Virtually immotile (56.8%, 25/44)	Stiff (18.2%, 8/44)	Restricted (15.9%, 7/44)	Circular (4.5%, 2/44)	Nearly normal (4.5%, 2/44)
Male sex*, %	50 (22/44)	44.0 (11/25)	37.5 (3/8)	71.4 (5/7)	50 (1/2)	100 (2/2)
Age, y	8.4	9.3	11.8	4.5	2	3.0
Laterality defect, %	68.1 (30/44)	68.0 (17/25)	87.5 (7/8)	71.4 (5/7)	0 (0/2)	50 (1/2)
NRDS*, %	56.4 (22/39)	61.9 (13/21)	50 (4/8)	33.3 (2/6)	100 (2/2)	50 (1/2)
Chronic wet cough*, %	83.3 (35/42)	91.7 (22/24)	75 (6/8)	66.7 (4/6)	50 (1/2)	100 (2/2)
Nasosinusitis*, %	100 (38/38)	100 (22/22)	100 (7/7)	100 (6/6)	100 (1/1)	100 (2/2)
Chronic otitis media*, %	96.7 (29/30)	100 (17/17)	83.3 (5/6)	100 (5/5)	NA	100 (2/2)
Hearing loss*, %	70.0 (21/30)	66.7 (12/18)	40.0 (2/5)	100 (3/3)	100 (2/2)	100 (2/2)
FEV_1,% pred	88.3	82.3	88.5	NA	NA	NA
Bronchiectasis*, %	34.2 (13/38)	36.4 (8/22)	62.5 (5/8)	0 (0/4)	0 (0/2)	0 (0/2)
Ciliary defect type, %	/	ODA/IDA (44.0%); ODA (28.0%); MTD/DA/CA (12.0%) Inconclusive (20.0%);	MTD/DA/CA (100%)	Normal (100.0%)	Normal/CA (100%)	Inconclusive (50%) Normal (50.0%)
Gene	/	*DNAH5;DNAHI1; CCDC103;DNAAF3 CCDC39;CCDC114*	*CCDC39;CCDC40 OFD1*	*DNAH11;DNAH5*	*HYDIN*	*DNAH11*

RGMC, reduced generation of multiple motile cilia; *NA*, Not applicable.
*Numerator/denominator, positive cases/total number of patients who underwent corresponding inspection.

complex system, or those involved in assembly and transport of the dynein arms (such as *DNAAF3, DNAAF1, DNAH5, DNAI1*, *CCDC114* and *CCDC103*), were identified in these subgroups. (2) Stiff cilia almost invariably showed IDA/MTD/CA defects. Among these children, genes associated with the factors of the nexin-dynein regulatory complexes (*CCDC39, CCDC40*) were identified. (3) Although TEM analysis of restricted cilia showed mostly normal ultrastructure, partial ODA defects and CA defects were occasionally observed. Pathogenic variants of the *DNAH5* and *DNAH11* genes were identified in this subgroup. (4) Mutations in *CCNO* resulted in greatly reduced number of cilia.

Although typical ciliary beat patterns can be attributed to genotype, it should be stressed that phenotypic variations can be found even within 1 gene. Among the exceptions, the individual P13, who carried a homozygous stop codon mutation in *CCDC*39 (NM_181426: c.526_527delCT), had completely static cilia. The individual P24, carrying the *DNAH5* (NM_001369: c.13126-2A>G; c.7789A>G) mutations, also exhibited a restricted beat pattern, which was distinct from the virtually immotile or minimal residual ciliary beating, reported in published PCD cases with *DNAH5* mutation.[35] These results highlight that the exact nature of the mutation in a given gene may have a distinctive effect on ciliary beating.[36]

To identify the genetic spectrum in Chinese patients with PCD, the related literature on gene variation of PCD were reviewed from Online Mendelian Inheritance in Man, HGMD, and PubMed up to July 2019 by using search terms of "primary ciliary dyskinesia," "gene," and "Chinese"; as a result, only 9 publications were found that reported a total of 19 Chinese cases of PCD, in which pathogenic genes were identified.[7-11] Collectively, a total of 63 cases (including 44 cases from the present study) of PCD were involved and analyzed. Taken together, the results revealed that *DNAH5* (25.4%), *DNAH11* (14.3%), *CCDC39* (12.7%), and *CCDC40* (11.1%) are the genetic basis of the majority of PCD cases, accounting for approximately 63.5% of the total. The genotypic spectrum identified in Chinese patients with PCD is also quite similar to that observed in Caucasians.

Diagnostic investigations of PCD are clearly complex, requiring expensive infrastructure and an experienced team of clinicians and scientists, which have restricted their scope of application. In fact, few studies have comprehensively evaluated the diagnostic accuracy and reliability of these tests. In the present study, we evaluated nNO, HSVA, TEM, and genetic tests in our cohort of children with PCD. As time-saving methods, nNO and HSVA have obviously higher diagnostic sensitivity, compared with TEM among our patients. Thus, the present study provides evidence for introducing nNO and HSVA into clinical practice as part of the diagnostic armamentarium for PCD. Moreover, as this study had a high yield of positive genetic diagnoses, many medical institutions without nNO and HSVA could benefit from genetic testing. Our results also suggest that great caution should be taken in interpreting genetic variants of uncertain significance. Some variants that disrupt splicing or redirect splicing at noncanonical sites may be mistaken for benign variants.[37]

Several limitations of this study deserve comment. First, there was potential for observer bias because the ciliary beating pattern analysis was largely based on a subjective description. Second, as there was significant heterogeneity of lung disease in different age groups, the sample size of our study is not powered to distinguish the clinical features between different beat pattern groups. However, we note that this study represents an initial effort to adequately diagnose and fully characterize these patients in China. Third, as a single-center study, we acknowledge that a selection bias was possible. PCD with laterality defects would more easily draw the doctor's attention and be diagnosed, which could have led to a high proportion of SIT among our patients.

In conclusion, by utilizing state-of-the-art diagnostic techniques, we provide a detailed description of the diversity of clinical manifestations, ciliary phenotypes, and genetic spectrum of a large cohort with PCD from China. Our study shows that a considerable proportion of patients with PCD had associated abnormalities. The genotypic spectrum and the unique genotype/ciliary phenotype correlation in Chinese are generally similar to that observed in Caucasians. We hope that the diversity of phenotypes and genotypes identified by this study will lead to better diagnosis for PCD and recognize the heterogeneous nature of this orphan disease. ■

Submitted for publication Dec 23, 2019; last revision received May 22, 2020; accepted May 26, 2020.

Reprint requests: Liling Qian, MD, PhD, Respirology Department, Children's Hospital of Fudan University, 399 Wan Yuan Rd, Shanghai 201102, P.R. China. E-mail: llqian@126.com

Data Statement

Data sharing statement available at www.jpeds.com.

References

1. Damseh N, Quercia N, Rumman N, Dell SD, Kim RH. Primary ciliary dyskinesia: mechanisms and management. Appl Clin Genet 2017;10:67-74.
2. Knowles MR, Daniels LA, Davis SD, Zariwala MA, Leigh MW. Primary ciliary dyskinesia. Recent advances in diagnostics, genetics, and characterization of clinical disease. Am J Respir Crit Care Med 2013;188:913-22.
3. Kuehni CE, Frischer T, Strippoli MP, Maurer E, Bush A, Nielsen KG, et al. Factors influencing age at diagnosis of primary ciliary dyskinesia in European children. Eur Respir J 2010;36:1248-58.
4. Lucas JS, Barbato A, Collins SA, Goutaki M, Behan L, Caudri D, et al. European Respiratory Society guidelines for the diagnosis of primary ciliary dyskinesia. Eur Respir J 2017;49:1601090.
5. Davis SD, Ferkol TW, Rosenfeld M, Lee HS, Dell SD, Sagel SD, et al. Clinical features of childhood primary ciliary dyskinesia by genotype and ultrastructural phenotype. Am J Respir Crit Care Med 2015;191:316-24.
6. Knowles MR, Ostrowski LE, Leigh MW, Sears PR, Davis SD, Wolf WE, et al. Mutations in RSPH1 cause primary ciliary dyskinesia with a unique clinical and ciliary phenotype. Am J Respir Crit Care Med 2014;189:707-17.
7. Xu X, Gong P, Wen J. Clinical and genetic analysis of a family with Kartagener syndrome caused by novel DNAH5 mutations. J Assist Reprod Gen 2017;34:275-81.

8. Sui W, Hou X, Che W, Ou M, Sun G, Huang S, et al. CCDC40 mutation as a cause of primary ciliary dyskinesia: a case report and review of literature. Clin Respir J 2016;10:614-21.
9. Guo T, Tan ZP, Chen HM, Zheng DY, Liu L, Huang XG, et al. An effective combination of whole-exome sequencing and runs of homozygosity for the diagnosis of primary ciliary dyskinesia in consanguineous families. Sci Rep 2017;7:7905.
10. Yang L, Banerjee S, Cao J, Bai X, Peng Z, Chen H, et al. Compound heterozygous variants in the coiled-coil domain containing 40 gene in a chinese family with primary ciliary dyskinesia cause extreme phenotypic diversity in cilia ultrastructure. Front Genet 2018;9:23.
11. Guo Z, Chen W, Huang J, Wang L, Qian L. Clinical and genetic analysis of patients with primary ciliary dyskinesia caused by novel DNAAF3 mutations. J Hum Genet 2019;64:711-9.
12. Liu L, Luo H. Whole-exome sequencing identified a novel compound heterozygous mutation of LRRC6 in a Chinese primary ciliary dyskinesia patient. Biomed Res Int 2018;1854269.
13. Wang K, Chen X, Guo CY, Liu FQ, Wang JR, Sun LF. Cilia ultrastructural and gene variation of primary ciliary dyskinesia: report of three cases and literatures review. Zhonghua Er Ke Za Zhi 2018 2;56:134-7.
14. Shen N, Meng C, Liu Y, Gai Z. Genetic diagnosis of a case with primary ciliary dyskinesia type 29 by next generation sequencing. Zhonghua Yi Xue Yi Chuan Xue Za Zhi 2019;36:225-8.
15. Chen LL, Yang YG, Wu JZ, Chen XR. Primary ciliary dyskinesia with HYDIN gene mutations in a child and literature review. Zhonghua Er Ke Za Zhi 2017;55:304-7.
16. American Thoracic Society, European Respiratory Society. ATS/ERS recommendations for standardized procedures for the online and offline measurement of exhaled lower respiratory nitric oxide and nasal nitric oxide, 2005. Am J Respir Crit Care Med 2005;171:912-30.
17. Beydon N, Chambellan A, Alberti C, de Blic J, Clement A, Escudier E, et al. Technical and practical issues for tidal breathing measurements of nasal nitric oxide in children. Pediatr Pulmonol 2015;50:1374-82.
18. Yang L, Kong Y, Dong X, Hu L, Lin Y, Chen X, et al. Clinical and genetic spectrum of a large cohort of children with epilepsy in China. Genet Med 2019;21:564-71.
19. Richards S, Aziz N, Bale S, Bick D, Das S, Gastier-Foster J, et al. Standards and guidelines for the interpretation of sequence variants: a joint consensus recommendation of the American College of Medical Genetics and Genomics and the Association for Molecular Pathology. Genet Med 2015;17:405-24.
20. Leigh MW, Hazucha MJ, Chawla KK, Baker BR, Shapiro AJ, Brown DE, et al. Standardizing nasal nitric oxide measurement as a test for primary ciliary dyskinesia. Ann Am Thorac Soc 2013;10:574-81.
21. Shapiro AJ, Davis SD, Ferkol T, Dell SD, Rosenfeld M, Olivier KN, et al. Laterality defects other than situs inversus totalis in primary ciliary dyskinesia: insights into situs ambiguus and heterotaxy. Chest 2014;146:1176-86.
22. Best S, Shoemark A, Rubbo B, Patel MP, Fassad MR, Dixon M, et al. Risk factors for situs defects and congenital heart disease in primary ciliary dyskinesia. Thorax 2019;74:203-5.
23. Noone PG, Leigh MW, Sannuti A, Minnix SL, Carson JL, Hazucha M, et al. Primary ciliary dyskinesia: diagnostic and phenotypic features. Am J Respir Crit Care Med 2004;169:459-67.
24. Crowley S, Holgersen MG, Nielsen KG. Variation in treatment strategies for the eradication of Pseudomonas aeruginosa in primary ciliary dyskinesia across European centers. Chron Respir Dis 2019;16:1-8.
25. Alanin MC, Nielsen KG, von Buchwald C, Skov M, Aanaes K, Høiby N, et al. A longitudinal study of lung bacterial pathogens in patients with primary ciliary dyskinesia. Clin Microbiol Infect 2015;21:1093.e1-7.
26. Maglione M, Bush A, Nielsen KG, Hogg C, Montella S, Marthin JK, et al. Multicenter analysis of body mass index, lung function, and sputum microbiology in primary ciliary dyskinesia. Pediatr Pulmonol 2014;49:1243-50.
27. Davis SD, Rosenfeld M, Lee HS, Ferkol TW, Sagel SD, Dell SD, et al. Primary ciliary dyskinesia: longitudinal study of lung disease by ultrastructure defect and genotype. Am J Respir Crit Care Med 2019;199:190-8.
28. Marthin JK, Petersen N, Skovgaard LT, Nielsen KG. Lung function in patients with primary ciliary dyskinesia: a cross-sectional and 3-decade longitudinal study. Am J Respir Crit Care Med 2010;181:1262-8.
29. Brown DE, Pittman JE, Leigh MW, Fordham L, Davis SD. Early lung disease in young children with primary ciliary dyskinesia. Pediatr Pulmonol 2008;43:514-6.
30. Werner C, Lablans M, Ataian M, Raidt J, Wallmeier J, Große-Onnebrink J, et al. An international registry for primary ciliary dyskinesia. Eur Respir J 2016;47:849-59.
31. Bukowy-Bieryllo Z, Rabiasz A, Dabrowski M, Pogorzelski A, Wojda A, Dmenska H. Truncating mutations in exons 20 and 21 of OFD1 can cause primary ciliary dyskinesia without associated syndromic symptoms. J Med Genet 2019;56:769-77.
32. Kennedy MP, Omran H, Leigh MW, Dell S, Morgan L, Molina PL, et al. Congenital heart disease and other heterotaxic defects in a large cohort of patients with primary ciliary dyskinesia. Circulation 2007;115:2814-21.
33. Goutaki ML, Meier AB, Halbeisen FS, Lucas JS, Dell SD, Maurer E, et al. Clinical manifestations in primary ciliary dyskinesia: systematic review and meta-analysis. Eur Respir J 2016;48:1081-95.
34. Kennedy MP, Noone PG, Leigh MW, Zariwala MA, Minnix SL, Knowles MR, et al. High-resolution CT of patients with primary ciliary dyskinesia. AJR Am J Roentgenol 2007;188:1232-8.
35. Raidt J, Wallmeier J, Hjeij R, Onnebrink JG, Pennekamp P, Loges NT, et al. Ciliary beat pattern and frequency in genetic variants of primary ciliary dyskinesia. Eur Respir J 2014;44:1579-88.
36. Blanchon S, Legendre M, Bottier M, Tamalet A, Montantin G, Collot N, et al. Deep phenotyping, including quantitative ciliary beating parameters, and extensive genotyping in primary ciliary dyskinesia. J Med Genet 2020;57:237-44.
37. Soens ZT, Branch J, Wu S, et al. Leveraging splice-affecting variant predictors and a minigene validation system to identify Mendelian disease-causing variants among exon-captured variants of uncertain significance. Hum Mutat 2017;38:1521-33.

Table I. Primers for polymerase chain reaction validation

Patient	Chromosome	CDS	Primer F (5′-3′)	Primer R (5′-3′)
P33	Intron7	c.931-8T>C	GATTGGGAATAACACAGAGTTTGA	CTTTCTCTTCTACAGACATGGTTTT

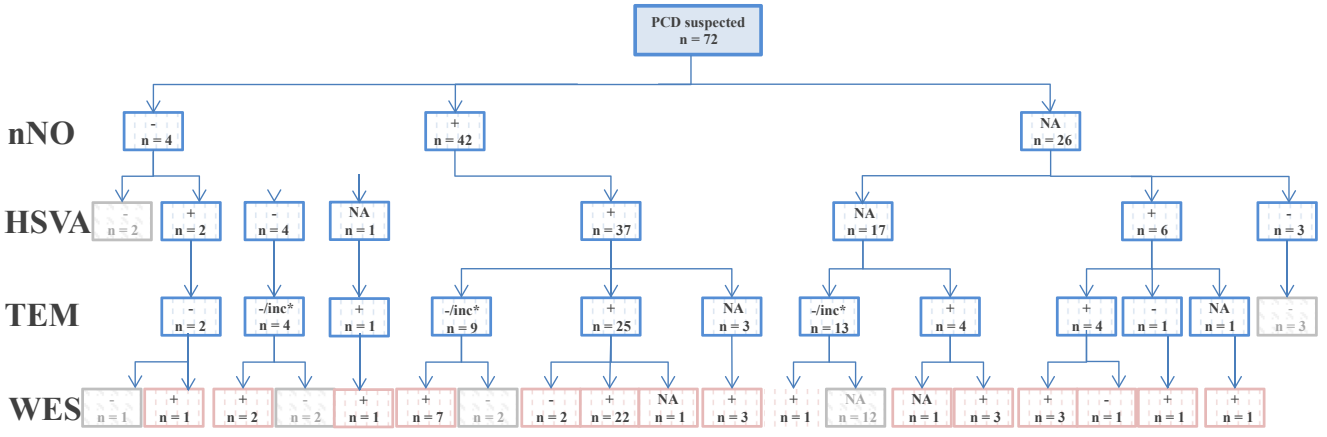

Figure 1. Flow chart of patient's enrollment and the diagnostic tests performed. *inc**, inconclusive; *NA*, not available.

Table III. Detailed clinical characteristics of the patients with PCD

Cases no	Sex	Age at enrollment	Age at diagnosis	RDS	Chronic cough	Sputum pathogens	Pulmonary function % pred			HRCT	Nasosinusitis	Otitis media	Hearing loss	Viscera situs	Other comorbidities
							FEV_1	FVC	FEF25–75						
P1	F	18	10	No	Yes	No	95.2	94.7	61.0	Diffuse nodules; Lobar atelectasis; Bronchiectasis;	Yes	NA	No	SIT	Dwarfism
P2	F	17	15.4	No	Yes	No	89.4	88.2	48.9	Diffuse nodules; Lobar atelectasis; Bronchiectasis	Yes	Yes	No	SIT	No
P3	M	11	0.1	Yes	Yes	No	88.3	114.1	66.0	Diffuse nodules; Bronchiectasis	Yes	Yes	Yes	SIT	No
P4	F	13	13	Yes	Yes	PA	73.7	65.2	22.4	Lobar atelectasis; Bronchiectasis	Yes	Yes	Yes	SIT	ACNA associated vasculitis
P5	F	10	10	No	Yes	No	82.9	61.6	27.1	Diffuse nodules; Lobar atelectasis; Bronchiectasis	Yes	NA	No	SIT	Thoracic deformity
P6	M	2.1	0.6	Yes	Yes	No	NA	NA	NA	Patchy exudation	Yes	Yes	Yes	SIT	NA
P7	F	5	5	Yes	Yes	NA	100.9	101.4	82.0	Lobar atelectasis; pleural effusion	Yes	Yes	NA	SS	No
P8	F	2	2	Yes	Yes	HI	NA	NA	NA	Diffuse nodules; Patchy exudation	Yes	Yes	Yes	SIT	No
P9	F	16	14.2	No	Yes	No	87.6	75.0	41.0	Diffuse nodules; Lobar atelectasis; Bronchiectasis	Yes	Yes	No	HTX	Anosmia
P10	F	10	9.8	Yes	Yes	HI	97.5	84.7	59.8	Patchy exudation; Diffuse nodules; Bronchiectasis	Yes	NA	No	SS	No
P11	M	1	1	Yes	Yes	NA	NA	NA	NA	Patchy exudation	Yes	Yes	Yes	SIT	No
P12	M	6	6	Yes	Yes	MC	84.7	80.1	41.6	Lobar atelectasis	Yes	Yes	Yes	SIT	Thoracic deformity
P13	M	7	7	Yes	Yes	MC	60.6	53.4	20.4	Patchy exudation; Diffuse nodules;	Yes	Yes	NA	SS	Thoracic deformity Dwarfism
P14	F	7	7	Yes	Yes	No	94.3	105.4	63.7	Lobar atelectasis;	Yes	Yes	Yes	SIT	No
P15	F	13	13	No	Yes	LP	NA	NA	NA	Diffuse nodules;	Yes	NA	Yes	SS	No
P16	F	2	0.8	Yes	Yes	No	NA	NA	NA	NA	NA	NA	NA	SIT	No
P17	M	3	3	Yes	Yes	NA	NA	NA	NA	Nearly normal	Yes	Yes	NA	SIT	No
P18	F	7	7	No	No	NA	106.3	100.4	93.2	Lobar atelectasis	Yes	Yes	NA	SS	No
P19	M	10	10	NA	NA	No	NA	NA	NA	NA	Yes	Yes	Yes	SIT	NA
P20	M	8	8	No	No	NA	NA	NA	NA	Nearly normal	NA	NA	Yes	SS	No
P21	M	17	17	NA	Yes	NA	85.2	70.6	34.0	NA	Yes	NA	NA	SIT	NA
P22	M	6	5.7	Yes	Yes	No	88.3	68.4	21.8	Diffuse nodules; Lobar atelectasis	Yes	Yes	Yes	SIT	No
P23	F	2	2	NA	NA	No	NA	NA	NA	NA	Yes	Yes	Yes	SIT	No
P24	M	5	5	No	No	NA	NA	NA	NA	NA	Yes	Yes	Yes	SIT	NA
P25	M	1	1	No	Yes	NA	NA	NA	NA	Nearly normal	Yes	Yes	Yes	SIT	No
P26	F	16	16	Yes	Yes	PA	NA	NA	NA	Diffuse nodules; Bronchiectasis	Yes	NA	NA	SIT	No
P27	M	9.8	9.8	NA	Yes	NA	81.1	82.3	62.7	Patchy exudation; Lobar atelectasis; Bronchiectasis;	NA	NA	NA	SIT	No
P28	M	6	6	No	Yes	No	NA	NA	NA	NA	Yes	Yes	NA	SS	NA
P29	M	17	15.2	NA	Yes	NA	NA	NA	NA	NA	Yes	NA	NA	SIT	No
P30	M	0.3	0	Yes	Yes	SA	NA	NA	NA	Nearly normal	NA	NA	Yes	SS	VSD,ASD
P31	F	10.9	10.4	Yes	Yes	NA	96.0	65.0	41.2	Diffuse nodules	Yes	Yes	Yes	SS	Congenital deafness
P32	M	4.9	4.4	Yes	Yes	No	NA	NA	NA	Patchy exudation	Yes	yes	Yes	SS	No
P33	F	18	17.3	No	Yes	PA	90.0	89.9	48.7	Diffuse nodules; Lobar atelectasis; Bronchiectasis	NA	NA	No	HTX	No
P34	M	12.1	6.7	Yes	Yes	HI,AB	83.5	92.5	43.1	Diffuse nodules; Lobar atelectasis; Bronchiectasis	Yes	Yes	No	SIT	VSD; Thoracic deformity
P35	M	17	17	No	Yes	NA	83.4	106.6	53.0	NA	Yes	NA	No	SIT	Atrial rhythm
P36	M	0.9	0.9	Yes	Yes	NA	NA	NA	NA	Patchy exudation; Lobar atelectasis	NA	NA	NA	SIT	No
P37	F	7.3	7.3	No	Yes	HI	85.6	80.7	28.4	Diffuse nodules; Lobar atelectasis	Yes	Yes	No	SIT	No
P38	F	0.5	0.5	Yes	No	NA	NA	NA	NA	Nearly normal	NA	NA	Yes	SS	No
P39	M	3.5	2,5	Yes	Yes	MC	NA	NA	NA	Lobar atelectasis	Yes	NA	Yes	SS	No

(*continued*)

Table III. Continued

Cases no	Sex	Age at enrollment	Age at diagnosis	RDS	Chronic cough	Sputum pathogens	Pulmonary function % pred			HRCT	Nasosinusitis	Otitis media	Hearing loss	Viscera situs	Other comorbidities
							FEV_1	FVC	FEF25–75						
P40	M	17	17	Yes	Yes	No	97.2	109.8	89.9	Patchy exudation; Lobar atelectasis	Yes	Yes	NA	SIT	No
P41	M	10.2	10.2	Yes	Yes	HI	72.7	68.2	42.4	Diffuse nodules; Lobar atelectasis; Bronchiectasis;	Yes	Yes	Yes	SS	No
P42	M	13.7	11.7	No	Yes	No	86.0	60.7	33.8	Diffuse nodules;	Yes	Yes	No	SS	No
P43	F	3.1	3.1	Yes	Yes	NA	NA	NA	NA	Nearly normal	Yes	Yes	NA	SIT	No
P44	M	3.8	3.8	No	No	NA	NA	NA	NA	Nearly normal	Yes	NA	NA	HTX	ASD,DCRV
P45	F	11.2	5.2	No	Yes	NA	NA	NA	NA	Diffuse nodules;	Yes	Yes	NA	SIT	No
P46	F	18	18	NA	Yes	PA, SA	NA	NA	NA	Diffuse nodules; Lobar atelectasis; Bronchiectasis;	Yes	Yes	Yes	SIT	No
P47	F	15	15	NA	Yes	No	NA	NA	NA	Diffuse nodules; Lobar atelectasis; Bronchiectasis;	NA	NA	NA	SIT	Thoracic deformity, scoliosis
P48	M	5	5	No	No	No	NA	NA	NA	Patchy exudation;	Yes	No	NA	SIT	NA
P49	M	10.3	10.3	No	No	NA	81.4	77.5	53.2	Diffuse nodules; Lobar atelectasis; Bronchiectasis;	Yes	Yes	Yes	SS	NA
P50	F	13.2	13.2	No	Yes	HI	NA	NA	NA	Diffuse nodules; Bronchiectasis;	Yes	NA	No	SIT	scoliosis

AB, Acinetobacter baumannii; *ASD*, atrial septal defect; *DCRV*, double chambered right ventricle; *F*, female; $FEF_{25\%-75\%}$, forced expiratory flow at 25% and 75% of the pulmonary volume; *HI*, *Haemophilus influenza*; *LP*, *Legionella pneumophila*; *M*, male; *MC*, *Moraxella catarrhalis*; *NA*, not available; *PA*, *Pseudomonas aeruginosa*; *RDS*, respiratory distress; SA, *Staphylococcus aureus*.

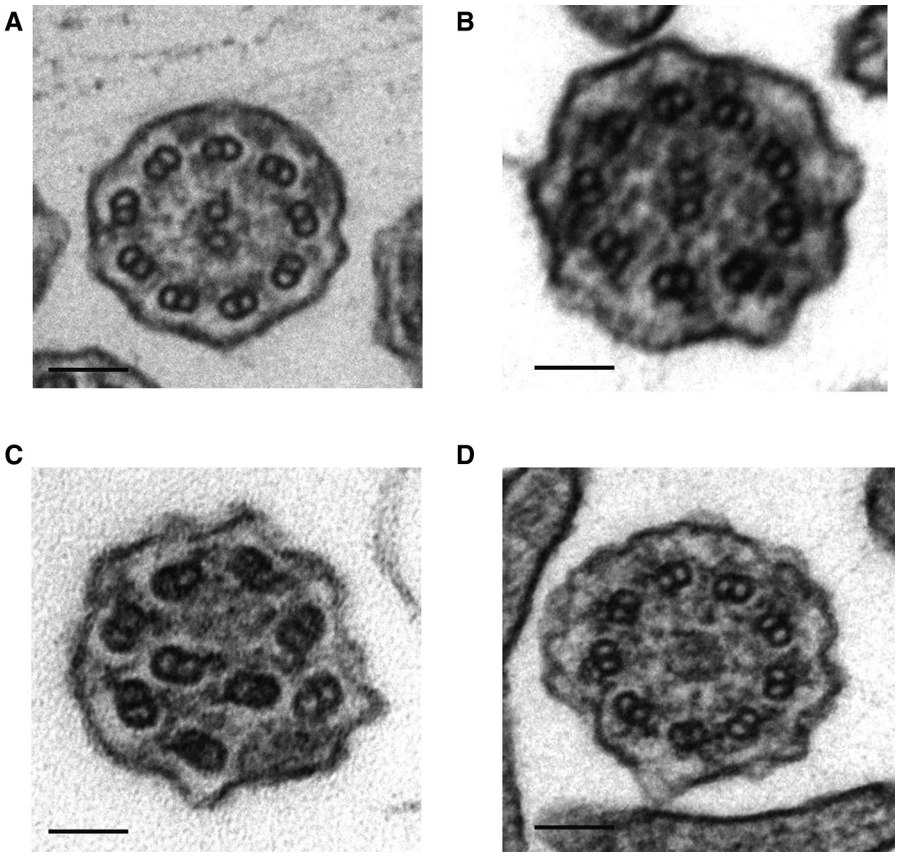

Figure 2. TEM images of PCD defects. **A,** ODA defect, **B,** IDA and ODA defect, **C,** dynein arm defects combined with microtubular disarrangement, and **D,** CA defect. Scale bar, 0.1 um.

Table V. Summary of diagnostic accuracy of nNO, TEM, HSVA, and WES in PCD

Parameters	nNO	TEM	CBP	CBF	WES
Available	39	46	44	38	48
Positive	38	33	42	30	45
Sensitivity	97.4%	71.7%	95.5%	78.9%	93.8%

CBF, cilia beat frequency; *CBP*, cilia beat pattern; *WES*, whole exome sequencing.

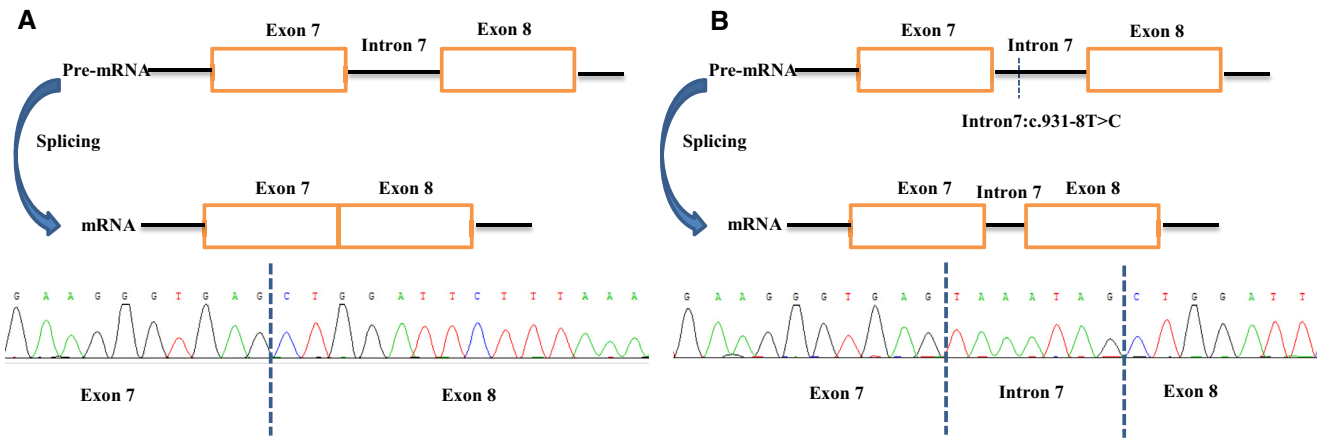

Figure 3. Schematic representation of *CCDC39* NM_181426: c.931-8T>C splicing. **A,** Schematic illustrating the normal splice of the *CCDC39* gene; there are no intron sequences between exons 7 and 8; **B,** Schematic illustrating the effect of the *CCDC39* mutation on the splice, causing an insertion of 7 bp of intron 7 in the cDNA sequence. The yellow boxes indicate the codon.